

Design of a Supercritical Fluid Expansion Source for Gas-Phase  
Spectroscopy of Fullerenes

Prospectus for Preliminary Examination

Department of Chemistry, School of Chemical Sciences

University of Illinois

Bradley M. Gibson

20 February 2013

271 RAL

2:00 PM

## I. Introduction

The fullerenes, including  $C_{60}$  and  $C_{70}$ , were discovered by Kroto *et al.* [1] in 1985 during experiments meant to simulate the chemistry of carbon stars. It was initially believed that these molecules would be formed primarily in carbon-rich, hydrogen-poor regions where formation of polyaromatic hydrocarbons (PAHs) would be limited. This hypothesis seemed to be supported by the first detection of extraterrestrial  $C_{60}$  and  $C_{70}$  by Cami *et al.* [2] in the planetary nebula Tc1, the remnant nebula of a carbon star, where no PAH emission features were detected. Later work by García-Hernández *et al.* [3] pointed out that Tc1 was not necessarily hydrogen-poor and also presented data showing fullerene and PAH emission features together in other planetary nebulae. They suggested that fullerenes may be formed through photochemical reactions of hydrogenated amorphous carbon grains. The precise mechanism by which fullerenes are formed in space is an active area of research [4,5,6]; obtaining high-resolution gas-phase spectra of  $C_{60}$  and  $C_{70}$  would allow astronomers to search for fullerenes in regions of space not accessible by emission spectroscopy and aid in accurate quantitation, potentially clarifying the formation process.

In addition to planetary nebulae, fullerenes have also been detected in the interstellar medium (ISM). Interstellar  $C_{60}$  was first detected by Sellgren *et al.* [7] in reflection nebulae via emission. They calculated that  $C_{60}$  could account for 0.1% to 0.6% of all interstellar carbon, but were hampered by uncertainties in its ultraviolet absorption cross-section. Absorption measurements could provide more precise estimates. In addition to the presence of neutral fullerenes in the ISM, relatively low ionization potentials mean that considerable quantities of ionized fullerenes could be present. Two features of the diffuse interstellar bands have been attributed to  $C_{60}^+$  by Foing and Ehrenfreund [8], although these have not been confirmed. An absorption spectrum of  $C_{60}^+$  could allow the claim to be confirmed or refuted, and solving the challenges of neutral fullerene spectroscopy would be the first step towards

obtaining the spectra of their molecular ions.

The primary challenges of gas-phase fullerene spectroscopy are low volatility and the substantial partition functions associated with such large molecules (see Fig. 1). Previous efforts in our group have focused on the production of C<sub>60</sub> vapor via high temperature oven and vibrational cooling through supersonic expansion [9]. This approach has failed largely due to the difficulty of cooling C<sub>60</sub> from such high initial temperatures. In response, I have developed a new supercritical fluid expansion (SFE) source for the production of cold fullerene vapor, based upon a similar source developed for supercritical fluid chromatography [10].

## II. Progress

### A. Results from High Temperature Oven Experiments

Initial attempts to observe C<sub>60</sub> utilized high-temperature ovens for vapor production and continuous-wave cavity ringdown spectroscopy (CW-CRDS) detection; the spectrometer (see Fig. 2) used a quantum cascade laser (QCL) centered at 1190 cm<sup>-1</sup>, and routinely achieved sensitivities of 10<sup>-8</sup> cm<sup>-1</sup> Hz<sup>-1/2</sup>. The most recent incarnation of the high temperature oven operated at temperatures between 955 and 965 K, initially vaporizing C<sub>60</sub> at a rate of 1.99 g/hr and later decreasing to a rate of 0.7 g/hr. The vapor was entrained in an argon flow with backing pressures ranging from 1.5 to 4 atmospheres and expanded through a 150 μm × 12.7 mm slit nozzle to provide cooling via supersonic expansion. The signal-to-noise ratio for the highest-intensity single rovibrational transition is given by

$$\frac{S}{N} = \frac{0.2 \times 0.515 \times N_{C_{60}} \times f \times S'}{2 \omega_0 \times v_{max} \times \Delta v \times \sigma_{NEA}}, \quad (1)$$

where  $N_{C_{60}}$  is the vaporization rate of C<sub>60</sub> in molecules/s,  $f$  is the fraction of C<sub>60</sub> in the ground vibrational state,  $S'$  is the calculated band strength in cm/molecule,  $\omega_0$  is the beam waist in cm,

$v_{max}$  is the flow velocity of molecules in the supersonic expansion in cm/s,  $\Delta\nu$  is the linewidth in  $\text{cm}^{-1}$  and  $\sigma_{NEA}$  is the noise-equivalent absorption. The leading coefficients account for the overlap of the supersonic expansion with the laser and the natural isotopic abundance of  $^{13}\text{C}$ . Assuming a linewidth of  $0.0004 \text{ cm}^{-1}$ , a rotational temperature of 20 K and a vibrational temperature of 0 K, estimated signal-to-noise ratios of 140 and 74 were calculated for the 1.99 g/s attempts and the 0.7 g/s attempt, respectively [9].

Despite relatively high estimated signal-to-noise ratios, no signal attributable to  $\text{C}_{60}$  was ever observed during the high temperature oven experiments. We believe this is due to inefficient vibrational cooling in our supersonic expansion and the high initial temperatures required. Estimates of linewidth and rotational temperature from earlier work with pyrene [11] should be reasonably accurate, and the vibrational temperature is the only remaining parameter that cannot be easily calculated. Based upon the highest signal-to-noise ratio for this oven, we can estimate that the vibrational temperature was 250 K or higher.

## B. Design of the Supercritical Fluid Expansion Source

Following these experiments, I set out to design a new source capable of producing  $\text{C}_{60}$  vapor at much lower temperatures. My current design (see Fig. 3) is based upon the sheath-flow SFE source developed by Sin *et al.* [10] for use with supercritical fluid chromatography. The sample, along with any co-solvent, is placed in a heated extraction chamber; liquid  $\text{CO}_2$  is then introduced and pressurized with an ISCO uL500 syringe pump. The supercritical fluid flows into a heated nozzle assembly and is depressurized through a  $10 \text{ }\mu\text{m}$  pinhole at a pressure-dependent flow rate of approximately  $3 \text{ }\mu\text{L/s}$ . The plume of depressurized fluid is then entrained in an argon sheath flow and expands through a heated  $150 \text{ }\mu\text{m} \times 12 \text{ mm}$  slit (see Fig. 4).

The effectiveness of this source for fullerene spectroscopy ultimately depends upon the amount of vapor that can be produced and the temperature of that vapor; these, in turn, will largely depend upon the solvent system chosen. Pure supercritical CO<sub>2</sub> is a poor solvent for C<sub>60</sub> and C<sub>70</sub>, but supercritical fluid extraction studies have shown that mixtures of supercritical CO<sub>2</sub> and toluene can be effective. Based upon work by Jinno and Kohrikawa [12], I estimate that a 7:3 mole fraction mixture of CO<sub>2</sub>:toluene should allow vapor production rates of 2.5 mg/hr at operating temperatures of 450 K. Increasing the toluene content could be expected to increase the vapor production rate at the cost of higher operating temperatures. Pure supercritical toluene would likely be an excellent solvent, but has a critical temperature of 592 K. A mixture of CO<sub>2</sub> and naphthalene could also prove effective – C<sub>60</sub> is approximately ten times more soluble in liquid naphthalene than in liquid toluene [13], and at 340 K can dissolve in supercritical CO<sub>2</sub> at a 96:4 CO<sub>2</sub>:naphthalene mole fraction [14]. It is not immediately clear what post-cooling vibrational temperatures these operating temperatures would correspond to, but pyrene has been shown to cool effectively from temperatures in excess of 420 K [11] and perylene has been shown to cool effectively from temperatures higher than 520 K [10].

### C. Initial Source Characterization

Initial tests of the source were carried out using supercritical CO<sub>2</sub> saturated with D<sub>2</sub>O. Issues with aerosol formation encountered by Sin *et al.* [10] led to some concern about the compatibility of the source with CRDS detection; in practice, however, no combination of source operating parameters has ever produced a detectable change in ringdown time constant. I monitored the 1<sub>11</sub>←0<sub>00</sub> rotational transition of the 010←000 vibrational band at 1199.793 cm<sup>-1</sup> as I varied the nozzle temperature and argon backing pressure. Signals were observed at nozzle temperatures between 400 K and 500 K and backing pressures of 1 to 60 psig. These tests were intended to characterize how the intensity of the

jet-cooled peak varied with changing conditions, but in most cases the signal exceeded the dynamic range of our instrument, making comparison difficult. A comparison of the jet-cooled signal to the background gas signal does show clear evidence of cooling, however (see Fig. 5). Furthermore, the observation of a jet-cooled peak for the  $1_{10}\leftarrow 1_{01}$  transition and the lack of such a peak for the  $2_{21}\leftarrow 3_{12}$  transition is indicative of rotational cooling; assuming a  $2_{21}\leftarrow 3_{12}$  peak was present at the level of our noise equivalent absorption, the rotational temperature would be approximately 16 K [15].

Given the difficulty of comparing the intensities of strong D<sub>2</sub>O transitions with our spectrometer, I next attempted to characterize the source through observations of the  $\nu_{68}$  band of pyrene. Pyrene was added to the source chamber along with toluene in amounts ranging from 5 mL to 40 mL; the source chamber was held at 3400 psi and 360 K. The lower toluene fraction runs exhibited consistent flow rates, but no pyrene signal was observed and little pyrene was observed to have collected inside the vacuum chamber. Runs using over 30 mL of toluene showed inconsistent flow rates, but resulted in significant deposition of pyrene onto the front plate of the vacuum chamber; no signal attributable to pyrene was observed during these runs either. This seems to suggest that the 10  $\mu$ m depressurization nozzle is becoming clogged intermittently. These issues persisted at nozzle temperatures ranging from 400 K to 500 K. Following these attempts to observe pyrene, I attempted to observe the  $\nu_8$  band of methylene bromide. Flow rates were inconsistent with methylene bromide as well, and no signal was observed. These results lead me to believe that the clogging issues are the result of multiple phases existing within the source; at present this cannot be confirmed.

Although the lack of a pyrene signal is disappointing, it is interesting to note that the pyrene collected on the front plate of the vacuum chamber spanned the height of the chamber but was approximately 1 cm wide. This is approximately the same width I have observed for pyrene residue collected inside the nozzle assembly when the expansion slit becomes clogged. This indicates that the depressurized supercritical fluid is confined to the center of the argon expansion, which should lead to

a smaller velocity spread and less Doppler broadening than would otherwise be observed [16].

### III. Future Work

#### A. Additional Source Characterization and Improvements

Although initial results with D<sub>2</sub>O were promising, later attempts with pyrene and methylene bromide revealed shortcomings of the current source which I will need to address. In particular, the extraction chamber heater cannot currently exceed 360 K and there is no simple way to check for the formation of multiple phases. I intend to correct these deficiencies by constructing a new source chamber. The heating deficiency is largely a result of poor thermal contact – the present chamber is simply a high-pressure steel tee, and its shape does not allow non-flexible heaters to be readily attached. As such, the new chamber will consist of a 1 inch diameter tube cut into a 2” × 2” × 5” stainless steel bar; the flat sides should allow good thermal contact with the 500 W strip heaters used in the first-generation C<sub>60</sub> oven. The ends of the tube will be capped with sapphire windows mounted in 1” NPT male fittings provided by Rayotek Scientific; additional NPT taps will be added along the top of the tube as needed to connect the rest of the source. These changes should allow the chamber to reach the temperatures necessary for producing toluene-rich supercritical fluids, while the addition of sight glasses should allow me to check for the formation of multiple phases and adjust operating parameters accordingly.

Following the construction of the new source chamber, I will resume my attempts to characterize the source through pyrene observations. The ultimate goal of these observations is to determine what combination of source conditions – including solvent composition, source temperature and pressure, nozzle temperature, argon backing pressure and expansion nozzle type – provides the maximum signal-to-noise ratio, then to estimate the rotational and vibrational temperatures of pyrene

under those conditions. For rotational temperature, this will be accomplished by observing multiple rovibrational transitions and preparing a Boltzmann plot. For vibrational temperature, it will be necessary to calculate the expected intensity of at least one rovibrational transition at the previously determined rotational temperature and compare the experimentally observed intensity. This further highlights the necessity of including windows in the source chamber design, as any undissolved pyrene in the source chamber would invalidate vapor production rate calculations.

Once vibrational and rotational cooling efficiency has been estimated through pyrene observations, I will experimentally determine the  $C_{60}$  and  $C_{70}$  vapor production rates. To do this, I will dissolve a sample of mixed  $C_{60}$  and  $C_{70}$  in the various solvent systems under consideration; the fluid will then be depressurized as normal, but with the argon flow line disconnected and the expansion slit replaced with a conflat blank. By washing the interior of the nozzle assembly with toluene and characterizing the resulting solution via mass spectrometry, it should be possible to estimate the amount of fullerene vapor produced. Although the flow rate through the depressurization pinhole is affected by the argon backing pressure, the effect is not significant at the relatively low pressures used [10] and should not significantly affect this estimate.

## B. Improving Instrument Sensitivity and Frequency Coverage

Following the characterization of the source, I should be able to estimate the sensitivity required to detect the fullerene vapor produced. For the 0.7 g/hr run with the high temperature  $C_{60}$  oven, the calculated absorption for the strongest rovibrational transition was  $5.5 \times 10^{-7} \text{ cm}^{-1}$ . Assuming a rotational temperature of 20 K, a vibrational temperature of 0 K and a vapor production rate of 2.5 mg/hr, the same transition can be expected to have an absorption of  $2.0 \times 10^{-9} \text{ cm}^{-1}$ . This calculation will obviously need to be adjusted once experimental values have been obtained, but provides a starting

point when considering the sensitivity required.

In its present form, our spectrometer (see Fig. 2) can routinely achieve sensitivities on the order of  $10^{-8} \text{ cm}^{-1} \text{ Hz}^{-1/2}$ . To detect the transition described above at a signal-to-noise ratio of 3, it would be necessary to signal average for 225 seconds per point; scanning at a typical rate of  $0.00025 \text{ cm}^{-1}$  per point, a  $1 \text{ cm}^{-1}$  scan would require approximately ten days of continuous scanning. Although cavity ringdown experiments can be run on such timescales by averaging many scans with more reasonable integration times [17], it would not be practical to do so with the SFE source I have described. As such, it will be necessary to increase the sensitivity of our spectrometer.

One option would be to implement high repetition rate ringdown collection. One method for achieving high repetition rates, described by Martínez *et al.* [18], is to actively lock the laser frequency to the ringdown cavity via the Pound-Drever-Hall (PDH) technique to enable more frequent buildup events and thus faster data collection rates. In this technique, a portion of the laser beam is directed through an electro-optic modulator to produce frequency sidebands and directed to a Fabry-Perot interferometer. The back reflection is then analyzed to produce an error signal, and frequency corrections are applied to lock the laser to the Fabry-Perot cavity. By matching the ringdown cavity to the Fabry-Perot cavity, ringdowns can be collected at rates in excess of 10 kHz. In our case, frequency corrections could be applied through our acousto-optic modulator and through current modulation of our QCL; although a gallium arsenide electro-optic modulator [19] could be used to generate sidebands, it may be preferable to produce these through current modulation as well. Given our current ringdown collection rate of approximately 100 Hz, we could expect a sensitivity of approximately  $10^{-9} \text{ cm}^{-1} \text{ Hz}^{-1/2}$  with this technique.

Alternatively, we could implement noise-immune cavity-enhanced optical heterodyne molecular spectroscopy (NICE-OHMS) detection. Although sensitivities as low as  $10^{-14} \text{ cm}^{-1} \text{ Hz}^{-1/2}$  have been reported for this technique [20], more typical values range from  $10^{-9} - 10^{-11}$ . NICE-OHMS detection

has been demonstrated with a QCL [21], with a reported sensitivity of  $10^{-10} \text{ cm}^{-1} \text{ Hz}^{-1/2}$ . Although NICE-OHMS may be required if vibrational cooling or fullerene vapor production are less effective than anticipated, implementing such a detection scheme would be complicated and expensive. If at all possible, high repetition rate ringdown will be used instead.

In addition to increasing the sensitivity of our spectrometer,  $C_{70}$  spectroscopy will require a light source with greater frequency coverage than our current QCL. To accomplish this, we will replace our current laser with an external cavity quantum cascade laser (EC-QCL) provided by collaborators in the Wysocki group. Our EC-QCL will use the Littrow configuration (see Fig. 6) and offer mode-hop free tuning [22] from  $1120 - 1250 \text{ cm}^{-1}$ . This should be sufficient to scan over several  $C_{70}$  vibrational bands.

### C. Spectroscopy of $C_{60}$ and $C_{70}$

Following these improvements to the source and spectrometer, we should have sufficient sensitivity and frequency coverage to allow high-resolution absorption spectroscopy of gas-phase  $C_{60}$  and  $C_{70}$ . In the case of  $C_{60}$ , we have chosen to search for the  $F_{1u}(3)$  vibrational band near  $1185 \text{ cm}^{-1}$  [23]. This is one of four infrared-active modes of the  $F_{1u}$  symmetry, and was chosen because it falls within an atmospheric transmission window, potentially allowing ground-based astronomical observations. In addition to the astrochemical importance of  $C_{60}$ , its rovibrational spectrum is also of fundamental interest. Because it is highly symmetrical and composed of bosons, its rotational motions are restricted – this will manifest as “missing” lines in its rovibrational spectrum [24] (see Fig. 7). As yet no experimental spectrum has had sufficient resolution to observe this.

In addition to  $C_{60}$ , we also wish to search for  $C_{70}$ . Three vibrational bands fall within the anticipated frequency coverage of our EC-QCL (see Fig. 8). The  $A_2''$  band near  $1140 \text{ cm}^{-1}$  is expected to be somewhat stronger than the  $1185 \text{ cm}^{-1}$  band of  $C_{60}$ , while the  $A_2''$  band near  $1205 \text{ cm}^{-1}$  and the  $E_1'$

band near  $1175\text{ cm}^{-1}$  are expected to be weaker [25]. As with  $C_{60}$ , these bands should be suitable for ground-based observations.

#### D. Additional Targets

In addition to its intended purpose of fullerene spectroscopy, it should be noted that the SFE source would also be well suited towards the study of large, low-volatility PAHs such as perylene and coronene. In addition to satisfying interest in interstellar PAHs, accurate absorption spectra could be useful when PAH absorption features occur near fullerene features. Most PAHs have at least one absorption band within the frequency coverage of our EC-QCL.

## IV. Conclusions

Despite the vast body of research centered upon the fullerenes  $C_{60}$  and  $C_{70}$  since their discovery, high-resolution gas phase vibrational absorption spectra have yet to be observed for either molecule. The absence of such spectra hinders efforts to observe these molecules in space, and prevents observations that could clarify how they are formed and their abundance in the ISM. The principal difficulties in obtaining these spectra are the low volatility and large partition functions of  $C_{60}$  and  $C_{70}$ . By developing a supercritical fluid expansion source capable of producing observable quantities of fullerene vapor at lower temperatures than have previously been possible, I hope to address these difficulties and observe the first cold gas-phase spectra of  $C_{60}$  and  $C_{70}$ , thus enabling new astronomical observations and clarifying the role of fullerenes in astrochemistry.

## References

- [1] H.W. Kroto, J.R. Heath, S.C. O'Brien, R.F. Curl and R.E. Smalley. *Nature* **318**, 162 (1985).
- [2] J. Cami, J. Bernard-Salas, E. Peeters and S.E. Malek. *Science* **329**, 1180 (2010).
- [3] D.A. García-Hernández, A. Manchado, P. García-Lario, L. Stanghellini, E. Villaver, R.A. Shaw, R. Szczerba and J.V. Perea-Calderon. *Astrophys. J. Lett.* **724**, L39 (2010).
- [4] O. Berné and A.G.G.M. Tielens. *Proc. Natl. Acad. Sci.* **109**, 401 (2012).
- [5] J. Bernard-Salas, J. Cami, E. Peeters, A.P. Jones, E.R. Micelotta and M.A.T. Groenewegen. *Astrophys. J.* **757**, 41 (2012).
- [6] D.A. García-Hernández, E. Villaver, P. García-Lario, J.A. Acosta-Pulido, A. Manchado, L. Stanghellini, R.A. Shaw and F. Cataldo. *Astrophys. J.* **760**, 107 (2012).
- [7] K. Sellgren, M.W. Werner, J.G. Ingalls, J.D.T. Smith, T.M. Carleton and C. Joblin. *Astrophys. J. Lett.* **722**, L54 (2010).
- [8] B.H. Foing and P. Ehrenfreund. *Nature* **396**, 296 (1994).
- [9] J.T. Stewart, B.E. Brumfield, B.M. Gibson and B.J. McCall. Submitted, (2013).
- [10] C.H. Sin, M.R. Linford and S.R. Goates. *Anal. Chem.* **64**, 233 (1992).
- [11] B.E. Brumfield, J.T. Stewart and B.J. McCall. *J. Phys. Chem. Lett.* **3**, 1985 (2012).
- [12] K. Jinno and C. Kohrikawa. *Chim. Oggi* **16**, 9 (1998).
- [13] R. Hidalgo-Quesada, X. Zhang and B.C. Giessen. *Mat. Res. Soc. Symp. Proc* **359**, 561 (1995).
- [14] S.T. Chung and K.S. Shing. *Fluid Phase Equilibria* **81**, 561 (1992).
- [15] C. Camy-Peyret, J.-M. Flaud, A. Mahmoudi, G. Guelachvili and J.W.C. Johns. *Int. J. Infrared Milli.* **6**, 199 (1985).
- [16] G. Scoles (Ed.), *Atomic and Molecular Beam Methods, Volume 1*, Oxford University Press (1988).
- [17] S. Kassi and A. Campargue. *J. Chem. Phys.* **137**, 234201 (2012).
- [18] R.Z. Martínez, M. Metsälä, O. Vaittinen, T. Lantta and L. Halonen. *J. Opt. Soc. Am. B* **23**, 727 (2006).

- [19] E. hirschmann and T. Walsh, Development of a 10.6-Micron Laser Modulator, NASA Technical Note (1966).
- [20] J. Ye, L.-S. Ma and J.L. Hall. *J. Opt. Soc. Am. B* **15**, 6 (1998).
- [21] M.S. Taubman, T.L. Myers, B.D. Cannon and R.M. Williams. *Spectrochim. Acta A* **60**, 3457 (2004).
- [22] G. Wysocki, R.F. Curl, F.K. Tittel, R. Maulini, J.M. Bulliard and J. Faist. *Appl. Phys. B* **81**, 769 (2005).
- [23] N. Sogoshi, Y. Kato, T. Wakabayashi, T. Momose, S. Tam, M.E. DeRose and M.E. Fajardo. *J. Phys. Chem. A* **104**, 3733 (2000).
- [24] R. Saito, G. Dresselhaus and M.S. Dresselhaus. *Phys. Rev. B* **50**, 15 (1994).
- [25] V. Schettino, M. Pagliai and G. Cardini. *J. Phys. Chem. A* **106**, 1815 (2002).
- [26] B.E. Brumfield, J.T. Stewart, S.L. Widicus Weaver, M.D. Escarra, S.S. Howard, C.F. Gmachl and B.J. McCall. *Rev. Sci. Instrum.* **81** 063102 (2010).

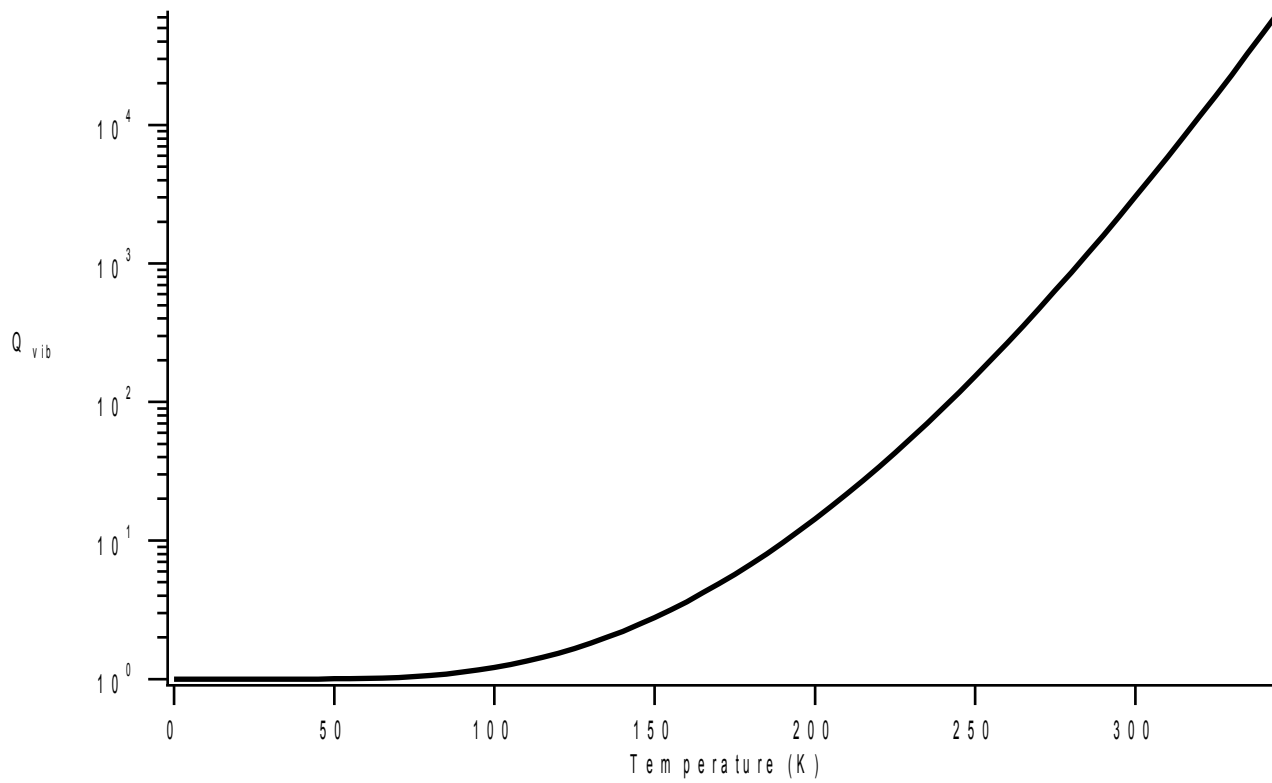


Figure 1: Log-scale plot of the vibrational partition function of  $C_{60}$  versus temperature. Adapted from [9].

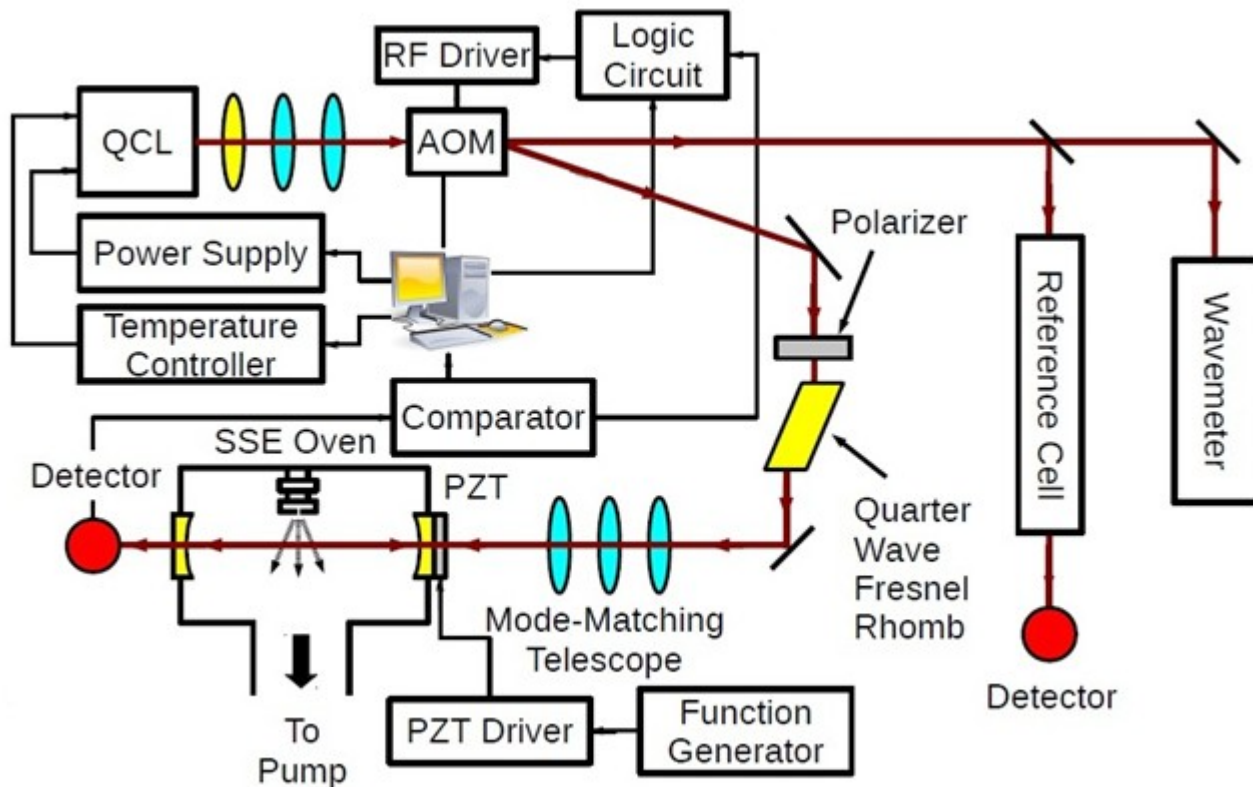


Figure 2: Block diagram of the existing CW-CRDS spectrometer. Light is generated by a Fabry-Perot QCL and directed towards an acousto-optic modulator (AOM). The zero-order diffracted beam is used for frequency calibration. The first-order diffracted beam is directed through a Fresnel rhomb backreflection isolator and a mode-matching telescope before being coupled into the ringdown cavity. As the intracavity intensity builds up, a comparator is triggered to turn off the AOM and allow ringdown to occur. Figure adapted from [26].

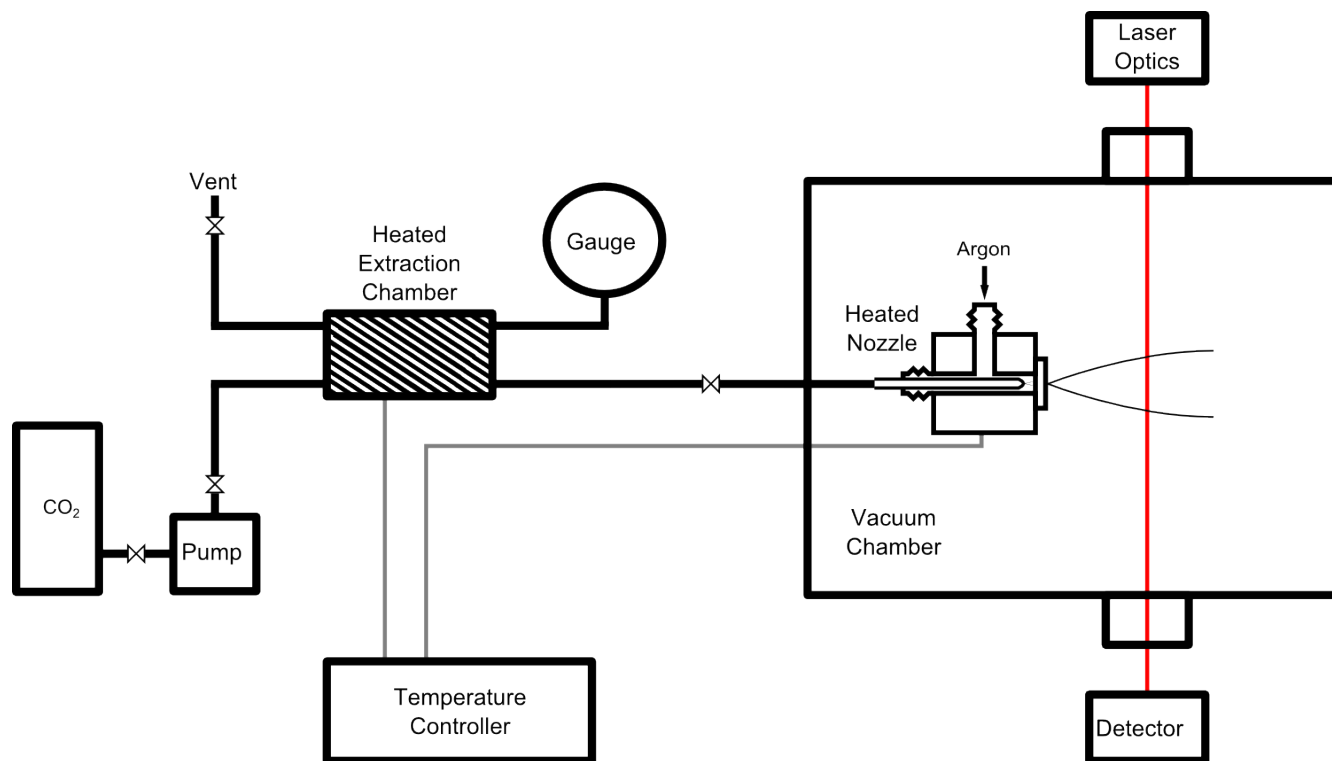


Figure 3: Block diagram of the SFE source. The sample and co-solvent are introduced to the heated extraction chamber. The chamber is then flooded with liquid CO<sub>2</sub> and pressurized by an ISCO uL500 syringe pump. The resulting supercritical fluid is depressurized through a 10 micron pinhole and entrained in an argon expansion as it flows through a 150 micron slit.

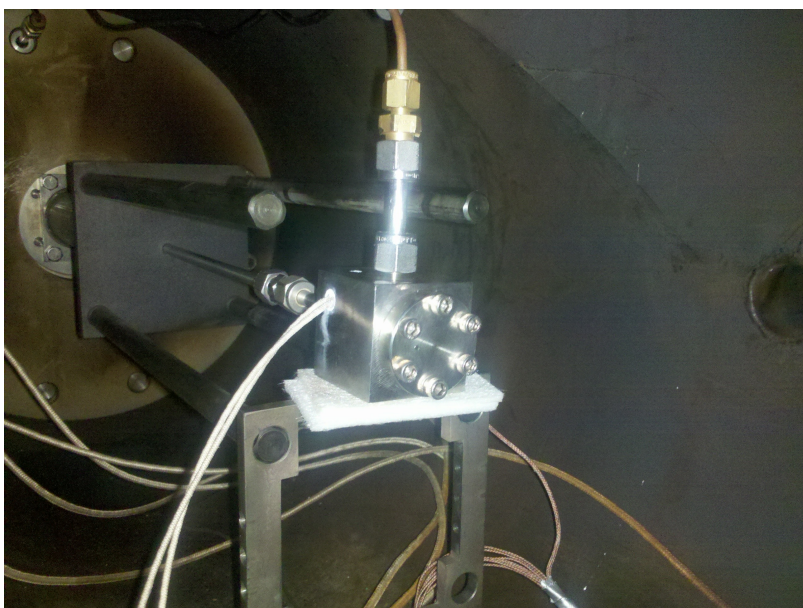


Figure 4: Photograph of the nozzle assembly.

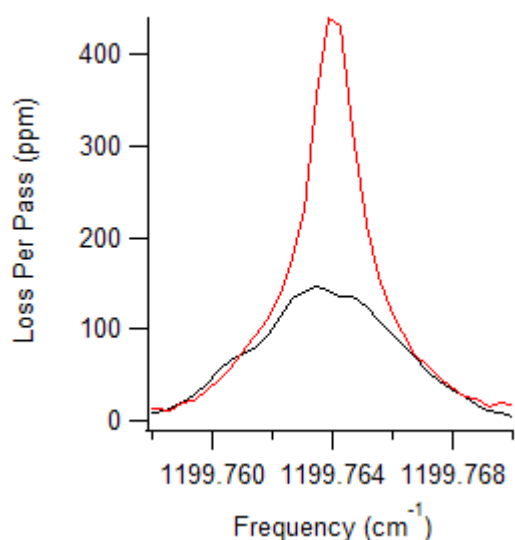


Figure 5: Sample scans of the  $1_{11} \leftarrow 0_{00}$  rotational transition of the  $(010) \leftarrow (000)$  vibrational band of  $D_2O$  at  $1199.793 \text{ cm}^{-1}$ . The black scan was taken without argon backing gas, and shows warm background gas in the chamber. The red scan was taken with argon backing gas, and shows a cooled jet signal on top of the background gas signal. The narrower linewidth is indicative of translational cooling, while the increased intensity is indicative of rotational or vibrational cooling. Note that the frequency is offset by the AOM; this can be corrected by comparison to a  $SO_2$  reference cell.

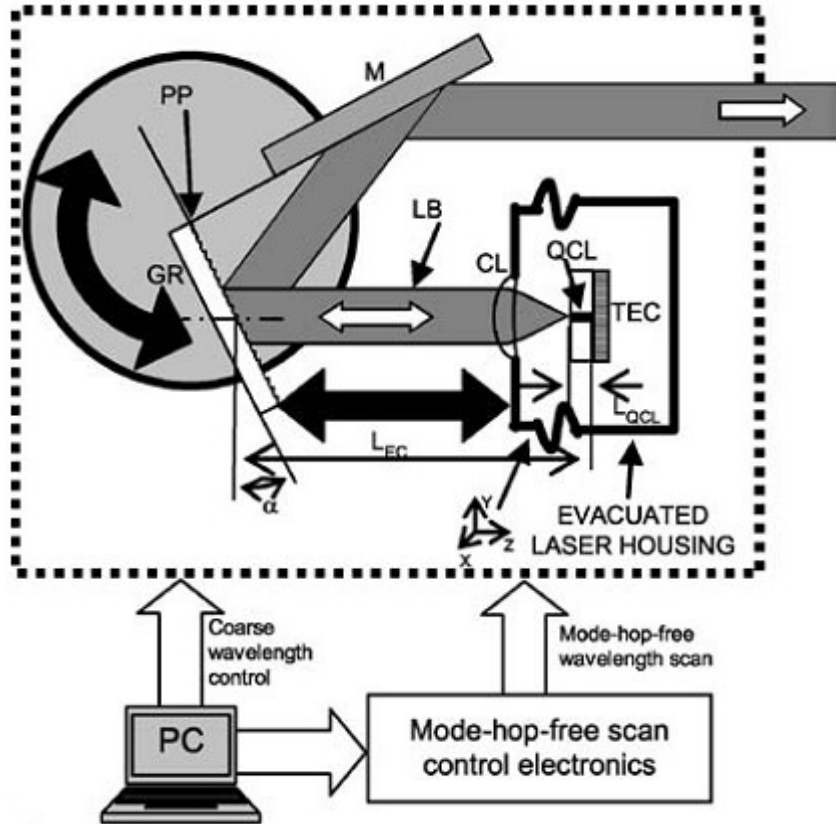


Figure 6: A Littrow-configuration EC-QCL. A diffraction grating mounted on a rotating stage acts as the output coupler for the laser cavity; the first-order diffracted beam is coupled back into the cavity while the zero-order diffracted beam is reflected out of the laser housing by a mirror mounted on the rotational stage. Properly aligned, this configuration allows the laser pointing to remain constant even as the rotational stage is adjusted to provide frequency tuning. The rotational stage is mounted on a horizontal translational stage, which provides another frequency tuning parameter. Figure adapted from [22].

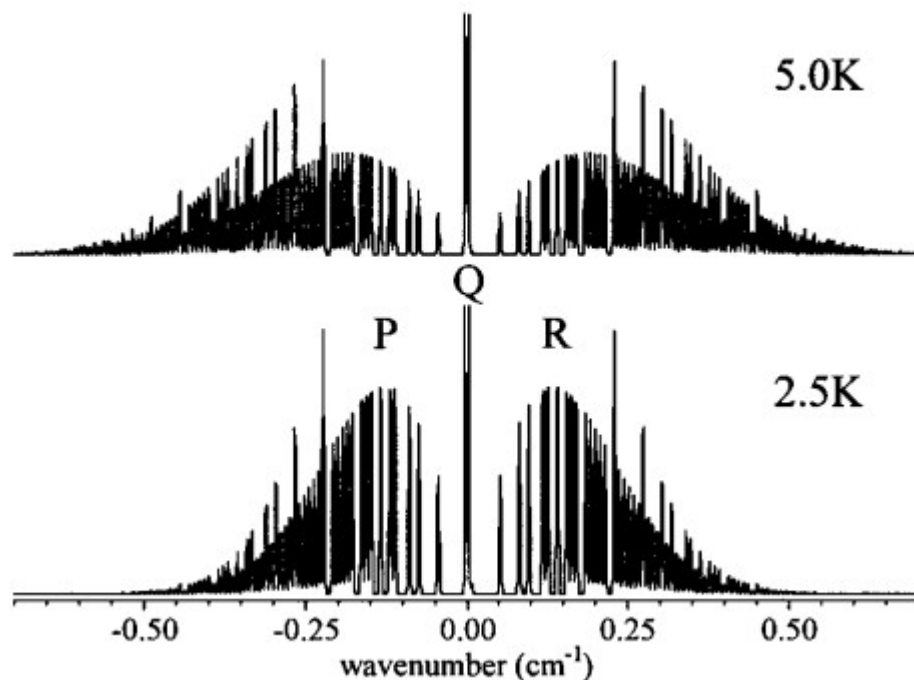


Figure 7: Calculated spectra of the  $F_{1u}(3)$  band of  $C_{60}$  at two rotational temperatures. The “missing” lines at low  $J$  values are due to symmetry restrictions on rotational motion. Figure from [23].

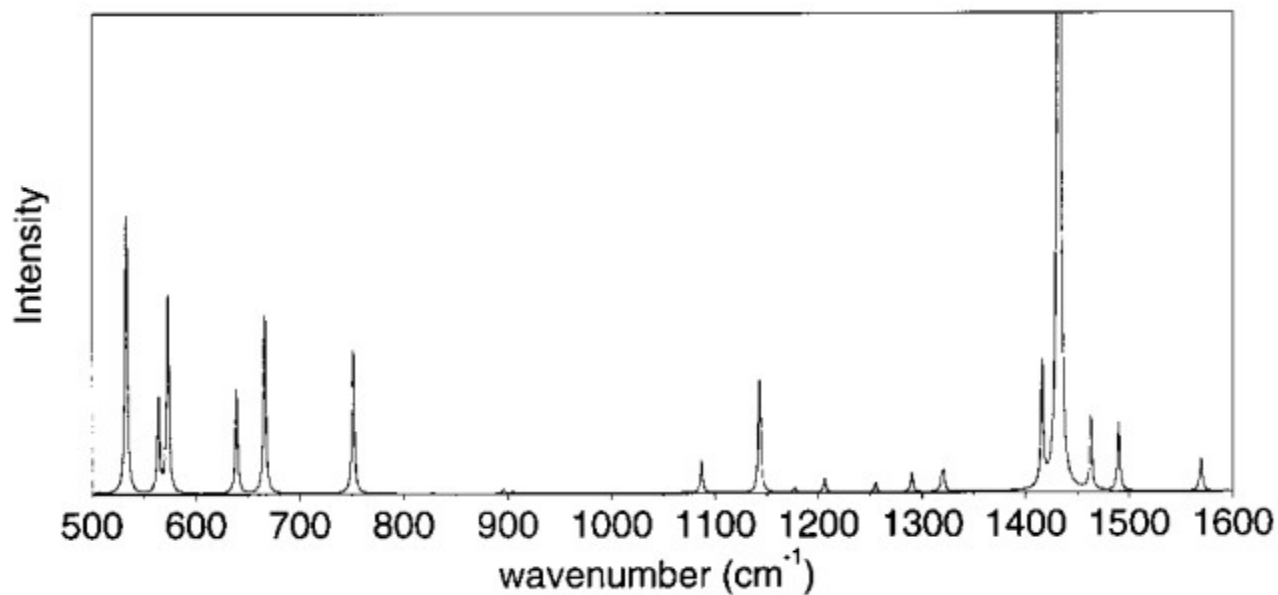


Figure 8: Calculated vibrational spectrum of  $C_{70}$ . Note the three bands which fall within our 1120-1250  $\text{cm}^{-1}$  tuning range. Adapted from [25].